A FREQUENCY-DOMAIN MODEL OF ELECTROMAGNETIC ACTUATORS COMPOSED OF SOLID IRON CORES WITH HYSTERESIS EFFECTS

FUKATA Satoru
Department of Industrial Design, Kyushu Institute of Design
4-9-1, Shiobaru, Minamiku, Fukuoka 815-8540, Japan
e-mail: fukata@kyushu-id.ac.jp

KOUYA Yoshinori
Murakami Seiki Mfg. Co., Ltd.
1-1, Kukikatamachi, Yahatanishiku, Kitakyushu 807-0811, Japan

FENG Shuang Ping
Graduate Student, Kyushu Institute of Design, Japan

SUMMARY

A model in the frequency domain is considered and checked with experimental results for the dynamic characteristics of magnetic actuators with solid iron core. First, an analytical magnetic reluctance based on a two-dimensional analysis is approximated in a simple form with a half-power of frequency and an accompanying complex number. This approximation is used to describe the dynamic characteristics of the electromagnet system with a C-shaped stator. Magnetic hysteresis effect is considered with a simple phase shift and with the conception of a complex value of permeability; leakage flux is ignored. The model is given by relations in the form of Laplace transform with the variation of working air-gap. For the symmetric electromagnet system with a uniform cross-sectional area, the frequency responses are compared with the experimental results when the working air-gap is fixed.

INTRODUCTION

When solid iron cores are used in electromagnets, eddy currents induced in the iron cores degrade and complicate the dynamic characteristics of the actuators. Several approaches have been presented to the analysis of eddy current effects, and distributive models have been derived (refs. 1-5). These are described by a transcendental function of the Laplace transform variable. There are two ways to obtain a lumped parameter model from the distributive models. One is to expand the transcendental functions into an infinite sum of lumped parameter systems and truncate them by several terms (refs. 6-8). The other one is to identify the parameters for a prescribed system in a range of frequency (ref. 9). The first method is very simple but may fail with a low-order system. The parameter identification method, in contrast, is generally reliable but requires a complicated computational procedure.

On the other hand, Feeley (ref. 10) proposed a simple distributive form to approximate an analytical one-dimensional model. This form is equivalent to the description with the half-power of the Laplace transform variable, $\sqrt{s}$. The approximation has been proven effective in very low and higher frequencies. This form may be useless in the time-domain analysis but presents few problems in the frequency-domain analysis. Britcher et al. (ref. 11) recommend an alternative form with a term such as $\sqrt{1+\tau s}$, where τ is a time constant.

In addition, magnetic hysteresis in iron cores has effects on the generation of the magnetic flux. The shape of the hysteresis loop is complex, in general; several models have been proposed in precise but very complicated forms (ref. 12). A simple treatment was devised by Aspden (ref. 1) with the conception of a complex value of permeability. This approach may have a difficulty in understanding the static hysteresis loop.

In this paper, we adopt an approximation similar to Feeley's and apply it to a theoretical magnetic reluctance of iron cores based on a two-dimensional analysis. With hysteresis effects, we take an approximated elliptical form for the static loop and apply it to the dynamic behaviors in its original form. The model considers the variation of working air-gap, but ignore's leakage flux. We check the validity of the proposed model with the experimental results when the working air-gap is fixed.

SYMBOLS AND NOTATIONS

A: Cross-sectional area of iron core.
a: Width of iron core.
B: Magnetic flux density.
b: Thickness of lamination.
b_m: Increment of B.
H: Magnetic field intensity in iron core.
H_s: H-value on the surface of iron core.
h_s: Increment of H_s.
I: Magnet-coil current.
i: Increment of I.
j: $= \sqrt{-1}$.
k_b: Gain of magnetic-flux density to coil current.
k_i: Gain of coil current to input voltage.
l_a: Mean length of air-gap.
l: Mean length of iron core.
N_k: Magnet-coil turns.
N: Total magnet-coil turns.
q: Incremental variable equivalent to magnetic flux.
R: Magnetic reluctance of iron core.
R_a: Magnetic reluctance of working air-gap.
r_a : Increment of R_a.
s: Laplace transform variable.
T: Time constant.
t : Time.
Φ: Magnetic flux.
ϕ: Increment of Φ.
μ : Permeability of iron core.
μ_0: Permeability of free space.
σ : Conductivity of iron core.
ω : Angular frequency.

APPROXIMATION OF MAGNETIC RELUCTANCE OF SOLID CORE

Assumptions

We make the following assumptions.
(A1) There is no leakage flux.
(A2) Magnetomotive force is uniform on the surface of iron core.
(A3) The distribution of magnetic flux is uniform in working air-gaps.
(A4) Magnetic material parameters are uniform and constant (no saturation).
(A5) The increments of flux and working air-gap are sufficiently small.

Eddy Current Effects

We consider a magnetic-flux path of length l and of constant cross-sectional area A, and assume the flux distribution is two-dimensional with assumption (A4). Eddy current effects complicate the flux distribution. We consider a rectangular iron core of width a and thickness b $(a \geq b)$. For the sinusoidal excitation of the magnetic intensity on the surface, a two-dimensional analysis derives the following equation as an expression of the amplitude of the induced flux (refs. 5 and 6).

$$\Phi(\omega) = \mu A H_s p(\omega) \tag{1}$$

where

$$p(\omega) = p_1(\omega) + p_2(\omega) \tag{2}$$

$$p_1(\omega) = \frac{\tanh(\alpha b/2)}{\alpha b/2} \tag{3}$$

$$p_2(\omega) = \sum_{k=1}^{\infty} \frac{8}{[(2k-1)\pi]^2} \frac{\alpha^2}{\beta_k^2} \frac{\tanh(\beta_k a/2)}{\beta_k a/2} \tag{4}$$

$$\alpha = \sqrt{j\mu\sigma\omega}, \qquad \beta_k^2 = \alpha^2 + \left[\frac{(2k-1)\pi}{b}\right]^2 \tag{5}$$

and where H_s is the amplitude of the input intensity on the surface, and ω an angular frequency. Equation (1) is rewritten as

$$H_s l = R(\omega)\Phi(\omega) \tag{6}$$

where

$$R(\omega) = \frac{R_0}{p(\omega)}, \qquad R_0 = \frac{l}{\mu A} \tag{7}$$

Approximation of Magnetic Reluctance

If the thickness is much smaller than the width ($b \ll a$), then the first term is dominant in eq. (2). To approximate this term, a low-order lumped parameter model is simple but not always successful because its series expansion has poor convergency. Feeley (ref. 10) proposed a distributive model described by the half-power frequency with the approximation

$$\tanh(x) \approx \frac{x}{1+x} \tag{8}$$

This approximation is very good in very low and high frequencies but fairly poor in the intermediate frequencies.

For real x, we note that the function $\tanh(x)/x$ monotonically decreases with increasing x. In this case, if we replace the second and higher-order terms by the first approximation, then we have an overestimation. Neglecting them, we have an underestimation. Taking the overestimation, we approximate the infinite sum of eq. (4) as

$$p_2(\omega) = \begin{cases} 0 & \text{for } \omega << \omega_{b1} \\ \dfrac{\tanh(\alpha a/2)}{\alpha a/2} & \text{for } \omega >> \omega_{b1} \end{cases} \tag{9}$$

where

$$\omega_{b1} = \frac{1}{\mu\sigma}\left(\frac{\pi}{b}\right)^2$$

In this case, for high frequencies, we have an approximation to eq. (2) as

$$p(\omega) \approx \frac{1}{\alpha b/2} + \frac{1}{\alpha a/2} = \left(1 + \frac{b}{a}\right)\frac{1}{\alpha b/2} \tag{10}$$

Considering the static value of unity, we give a rough approximation to the magnetic reluctance as

$$\frac{R(\omega)}{R_0} \cong \bar{r}_2(\omega) = 1 + \alpha\frac{b'}{2}, \qquad b' = \frac{b}{1 + \dfrac{b}{a}} \tag{11}$$

To check the approximation, we take up a iron core of a =20mm and b =8mm (b/a =0.4) with the material parameters in Table 1 given later. The absolute value and argument are shown in Fig. 1 by broken lines (notation $\bar{r}_2$), and compared with the theoretical values shown by thick filled lines ($\bar{r}_0$). The approximation is very good in higher frequencies but fairly poor in lower frequencies. The comparison for different values of width and material parameters is given only against a scaled frequency axis. The approximation becomes better with the increase of the ratio b/a (≤ 1).

To improve the approximation in lower frequencies, we may modify eq. (11) as

$$\bar{r}_3(\omega) = \frac{1}{1 + \dfrac{b}{a}}\left(1 + \alpha\frac{b}{2}\right) \tag{12}$$

by ignoring the accuracy in the statics. The evaluation is shown by thin filled lines with $\bar{r}_3$ in Fig. 1. This modification improves the first approximation in lower frequencies but is poor in very low frequencies. We note $\bar{r}_3(0) = 1/(1 + b/a) < 1$, while the first approximation gives the accurate value of unity.

The frequency characteristics with fixed working air-gap may be expressed by the transfer function

$$G(s) = \frac{1}{1 + c_{R0}\bar{r}(s)}, \qquad c_{R0} = \frac{R_0}{R_{a0}} \tag{13}$$

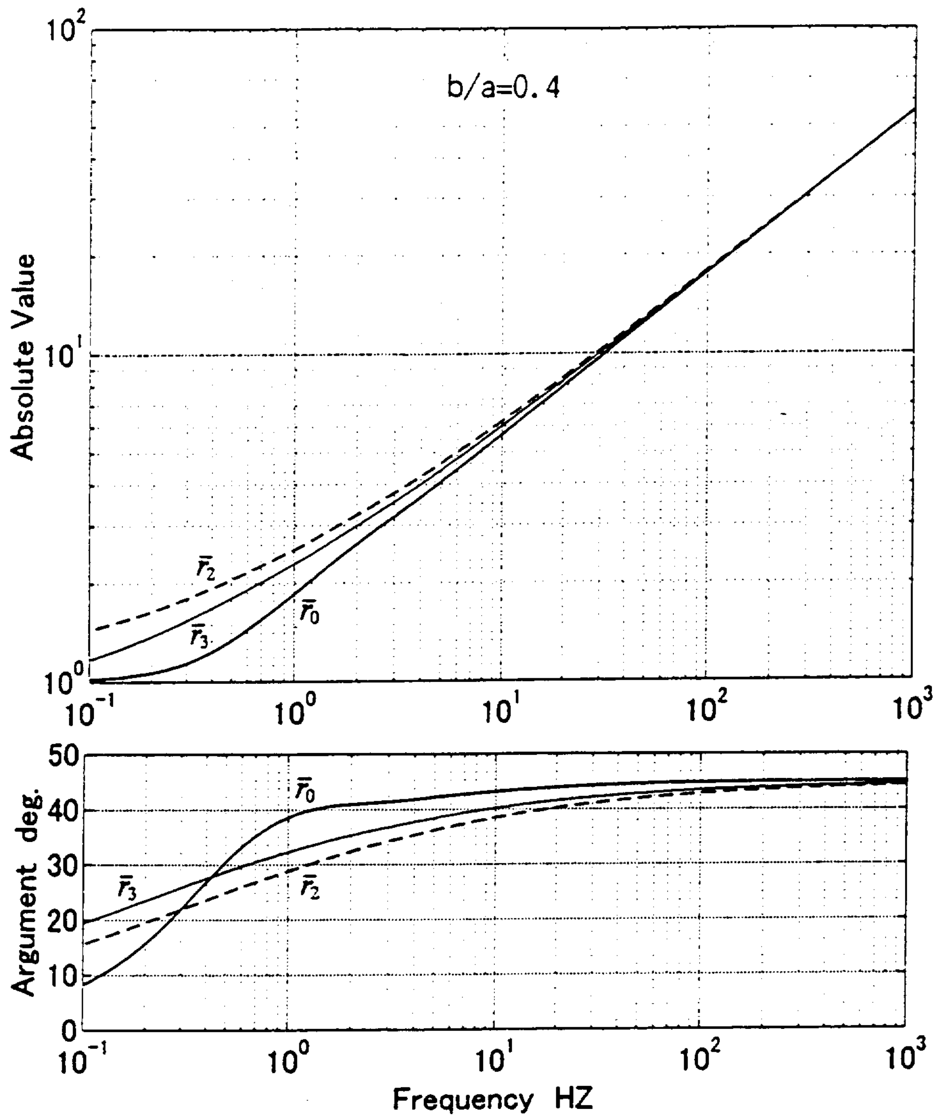

Figure 1. Approximation of magnetic reluctance.

In the equation, R_0 is the static magnetic reluctance of iron core and R_{a0} that of working air-gap. Figure 2 shows the frequency responses for the approximations when c_{R0} =0.1.

MODEL OF ELECTROMAGNETIC ACTUATORS WITH C-SHAPED STATOR

Magnetic Circuit Model

Figure 3 illustrates in the left-hand part a configuration of electromagnetic actuators composed of a C-shaped stator and an I-shaped rotor. Two coils are set on the two pole legs and connected in series. Actually, the magnetic flux is distributive with leakage along the flux path. When the effects of eddy currents are combined, the leakage fluxes increase with frequency; hence the dynamics become more complicated.

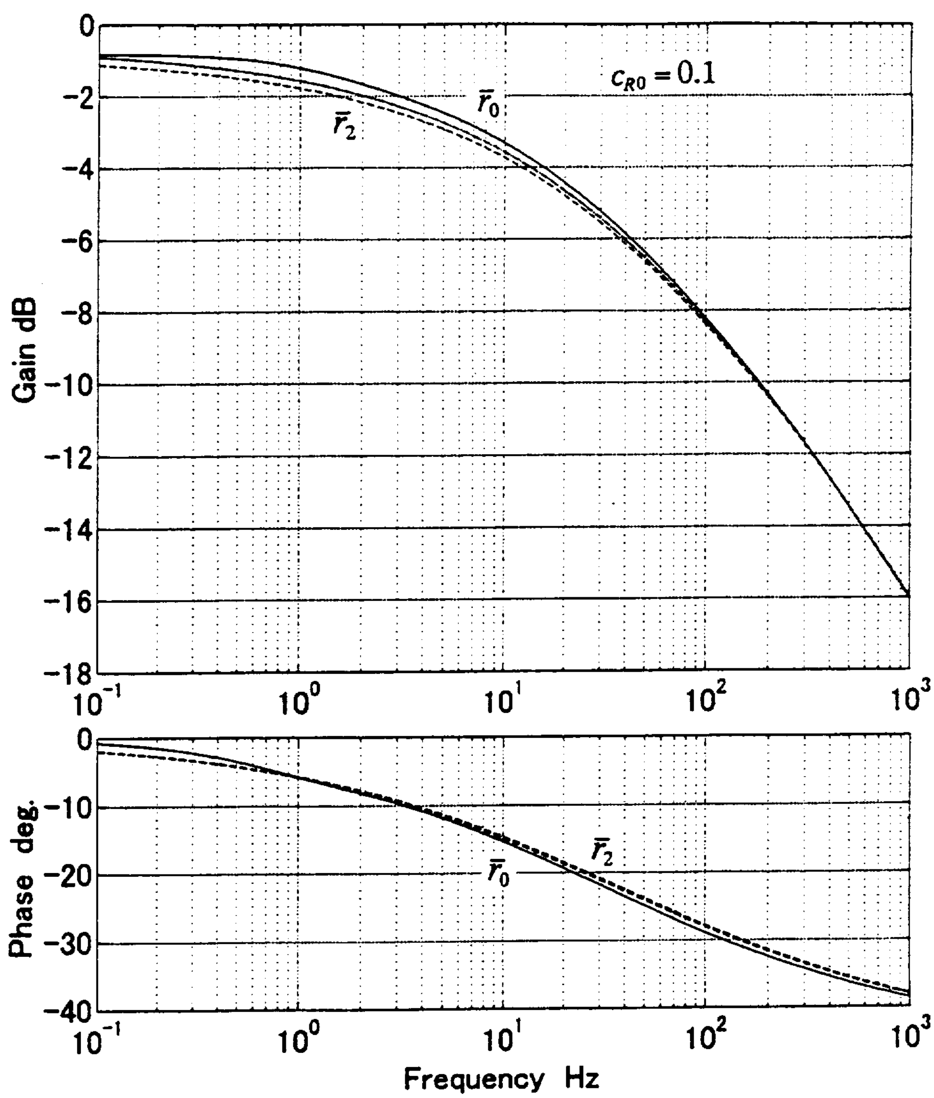

Figure 2. Frequency characteristics with approximated reluctance.

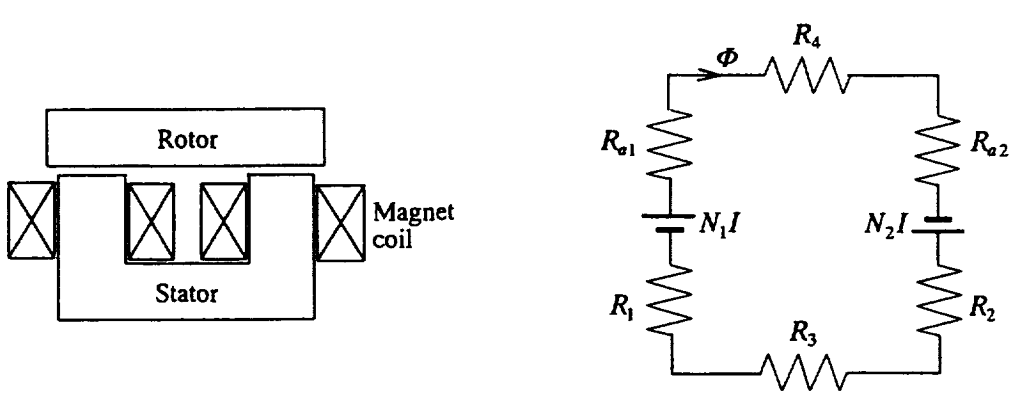

Figure 3. Configuration of magnetic actuator and magnetic circuit model.

If we neglect the leakage fluxes, the magnetic system is modeled by an equivalent magnetic circuit, as shown in the right-hand part of Fig. 3. In this figure, $N_k I$ are the magnetomotive forces, and R_{ak} and R_k are the magnetic reluctances in the working air-gaps and in the iron cores, respectively.

Relation of Magnetic Flux to Coil Current

For a loop along the surface of the iron cores in the magnetic system, Ampere's loop law gives the relation

$$H_a l_a + H_s l = NI \tag{14}$$

where H_a and l_a are the field intensity and the path length, respectively, associated with the working air-gap, H_s and l are those with the iron cores, N the turns of magnet coil and I the coil current. The length l is given by the mean on Assumption (A2). Concerning the working air-gap, with Assumption (A3) we have the relation

$$H_a l_a = R_a \Phi \tag{15}$$

where

$$R_a = \frac{l_a}{\mu_0 A_a}, \qquad \Phi = A_a B_a$$

where A_a is an effective area of the working air-gap, B_a the flux density assumed to be uniform over the area, and μ_0 the permeability of air. Concerning the iron cores, in the steady state, the flux distribution is uniform; hence, we have the simple relation

$$H_{s0} l = R_0 \Phi_0, \qquad R_0 = \frac{l}{\mu A} \tag{16}$$

where A is the cross sectional area and μ the permeability. This gives the steady-state value of the flux. In the unsteady state, another approach is required.

For the increment of coil current and for the variation of working air-gap length, we consider the resulting increments of the field intensity and the flux.

$$I = I_0 + i, \qquad R_a = R_{a0} + r_a, \qquad H_s = H_{s0} + h_s, \qquad \Phi = \Phi_0 + \phi \tag{17}$$

Substituting these into eq. (14) with eqs. (15) and (16) and neglecting the second-order term, $r_a \phi$, we obtain the equation of the increments

$$R_{a0}\phi + h_s l = Ni - \Phi_0 r_a \tag{18}$$

The Laplace transform of the above relation is given by

$$R_{a0}\phi(s) + h_s(s) l = Ni(s) - \Phi_0 r_a(s) \tag{19}$$

where the variables with the argument s denote the Laplace transform of the corresponding variable, for example, $\phi(s)$ of ϕ, with the initial values of zero.

Now, we apply the result of eq. (1) to eddy current effects in the magnet core. In a similar way to the derivation of eq. (1), from the Laplace transform of the original equation under some conditions for the associated functions, we can obtain a similar equation

$$R(s)\phi(s) = lh_s(s) \tag{20}$$

where $R(s)$ is given by the relation in eq. (7) where $j\omega$ is replaced by s in the term α in eq. (5). We set the initial values of the variables to be zero. Then, eq. (19) results in

$$\left[R_{a0} + R(s)\right]\phi(s) = Ni(s) - \Phi_0 r_a(s) \tag{21}$$

If we use a variable for the flux, defined by

$$q = \frac{R_{a0}}{N}\phi \tag{22}$$

then eq. (21) is written by

$$\left[1 + \bar{r}(s)\right] q(s) = i(s) - I_0\bar{r}_a(s) \tag{23}$$

where

$$\bar{r}(s) = \frac{R(s)}{R_{a0}}, \qquad \bar{r}_a = \frac{r_a}{R_{a0} + R_0} = \frac{1}{1+\bar{r}_0}\frac{r_a}{R_{a0}}, \qquad \bar{r}_0 = \frac{R_0}{R_{a0}} \tag{24}$$

and where we used the steady-state relation in the term with $\bar{r}_a(s)$.

Equations with Input Voltage

We take a power amplifier with coil-current control. In this case, the electric circuit gives an equation to the incremental voltage between the ends of magnet coil, v, as

$$v = p(k_i' e - i) = R_C i + N\frac{d\phi}{dt} \tag{25}$$

where e is an incremental voltage input to the power amplifier, k_i' a constant, p the loop gain of current feedback, and R_c the resistance of the magnet coil. Then, the above equation is simplified with eq. (22) as

$$i + T_0\frac{dq}{dt} = k_i e \tag{26}$$

where

$$k_i = \frac{pk_i'}{p + R_C}, \qquad T_0 = \frac{N^2}{(p + R_C)R_{a0}}$$

Substituting the Laplace transform of eq. (26) into eq. (23), we obtain the relation between the magnetic flux and the input voltage

$$\left[1 + Ts + \bar{r}(s)\right] q(s) = k_i e(s) - I_0\bar{r}_a(s) \tag{27}$$

For the coil current, we have

$$\left[1 + T_0 s + \bar{r}(s)\right] i(s) = \left[1 + \bar{r}(s)\right] k_i e(s) + I_0 T_0 s \bar{r}_a(s) \tag{28}$$

Effects of Magnetic Hysteresis

The conception of complex permeability allows us to consider the hysteresis effects with an approximate elliptical relation (ref. 1). This approach is simple and can be applied to the results obtained above only by use of the complex permeability $\mu e^{-j\theta}$ in place of the real permeability μ. This approach, however, presents difficulties with regard to giving a reasonable understanding to the experimental static hysteresis.

If we slowly change the value of magnet-coil current I with amplitude i_0 around a bias current I_0, then the magnetic flux forms a hysteresis loop with the current. Concerning the magnetic flux density, B_0 is the mean value of the upper and lower values at the bias current and b_{m0} the resulting amplitude. With the increments i and b_m around I_0 and B_0, respectively, we approximate the hysteresis loop with the elliptical function and consider the transfer function with a phase shift

$$\frac{b_m(s)}{i(s)} = k_b e^{-j\varphi} \tag{29}$$

where the phase shift φ determines the swell of the ellipse; φ =0 gives the linear relation $b_m = k_b i$, where k_b is the gradient of the long axis and given by

$$k_b = \frac{b_{m0}}{i_0} \tag{30}$$

The hysteresis loop brings another effect, in general, that the current-flux gain k_b varies with the variation of the amplitude of coil current. In the steady states without hysteresis effects, eq. (21) gives the flux $\phi_{TH}(s)$

$$\frac{\phi_{TH}(s)}{A_a} = k_{TH}\left[i(s) - \frac{\Phi_0}{N} r_a(s)\right], \qquad k_{TH} = \frac{N}{(R_{a0} + R_0)A_a} = \frac{\mu_0 N}{(1 + \bar{r}_0)l_a} \tag{31}$$

The term in the square brackets in the above equation is a magnetomotive force, corresponding to the coil current in eq. (29). Hence, a corresponding equation with the hysteresis effects is written by a similar form

$$\phi(s) = \bar{k}_b e^{-j\varphi} \phi_{TH}(s), \qquad \bar{k}_b = \frac{k_b}{k_{TH}} \tag{32}$$

Combining eq. (32) with eq. (21), we have the equations

$$\left[1 + \bar{r}(s)\right] q(s) = \bar{k}_b e^{-j\varphi}\left[i(s) - I_0 \bar{r}_a(s)\right] \tag{33}$$

$$\left\{\left[1 + \bar{r}(s)\right] e^{j\varphi} + Ts\right\} q(s) = \bar{k}_b\left[k_i e(s) - I_0 \bar{r}_a(s)\right] \tag{34}$$

$$\left[1 + \bar{r}(s) + Tse^{-j\varphi}\right] i(s) = \left[1 + \bar{r}(s)\right] k_i e(s) + I_0 Tse^{-j\varphi} \bar{r}_a(s) \tag{35}$$

where

$$T = \bar{k}_b T_0 \tag{36}$$

We note that the time constant T_0 was replaced by $\bar{k}_b T_0$. This is a result of the decay of back electromotive force in the magnet coil.

Special Case with Fixed Working Air-gap

The approximations of magnetic reluctance are applicable to iron cores composed of different cross-sectional dimensions or different materials. If the material and the dimensions are common, then the total reluctance has a simple form. When the working air-gap is fixed, i.e. $\bar{r}_a(s)=0$, if eq. (11) is applied to the magnetic reluctance of the iron core, then eqs. (33) to (35) are written by the very simple transfer functions:

$$\frac{q(s)}{i(s)} = \frac{\bar{k}_b e^{-j\varphi}}{1+\bar{r}_0\left(1+\sqrt{\tau s}\right)} \tag{37}$$

$$\frac{i(s)}{e(s)} = k_i \frac{1+\bar{r}_0\left(1+\sqrt{\tau s}\right)}{1+\bar{r}_0\left(1+\sqrt{\tau s}\right)+Tse^{-j\varphi}} = \frac{k_i}{1+\dfrac{Ts}{1+\bar{r}_0\left(1+\sqrt{\tau s}\right)}e^{-j\varphi}} \tag{38}$$

$$\frac{q(s)}{e(s)} = \frac{k_i \bar{k}_b e^{-j\varphi}}{1+\bar{r}_0\left(1+\sqrt{\tau s}\right)+Tse^{-j\varphi}} \tag{39}$$

where τ is a time constant given by

$$\sqrt{\tau} = \frac{1}{1+b/a}\sqrt{\mu\sigma}\frac{b}{2} = \sqrt{\mu\sigma}\frac{b'}{2} \tag{40}$$

EXPERIMENTAL RESULTS

Experimental Setup

Figure 3 shows the dimensions of the magnet-iron cores; the cross-sectional area perpendicular to the flux path is uniform. The rotor is longer by 5mm than the width of the stator, and sticks out by 2.5mm from the pole legs on each side. The material is a soft iron. The magnet coils have the same turns and are excited with a PWM power amplifier with current feedback control. Two pieces of cardboard are put between the pole-leg faces and the rotor core to set the working air-gap length. We set the air-gaps to 1mm and the bias current to 1.5A. The primary specifications and data are summarized in Table 1.

Magnetic Hysteresis Loop

Hysteresis loop of the flux density against the coil current was measured with a gaussmeter in the working air-gap when the coil current was changed through the input voltage with the bias current. To obtain the static hysteresis loop, we applied a sinusoidal input at a frequency of 0.0125Hz, and had the data of two periods. The results are shown in Fig. 4 for three amplitudes; the hysteresis is very small. The loops are approximated with a phase shift of about φ =0.03rad. (=1.7 deg.) in eq. (29). This phase shift is so small that we will neglect it in the calculations below. The argument of permeability, θ, has a small effect on the static loop when we calculate it with eq. (37). Hence, it may be difficult to estimate the value of θ from the static loop.

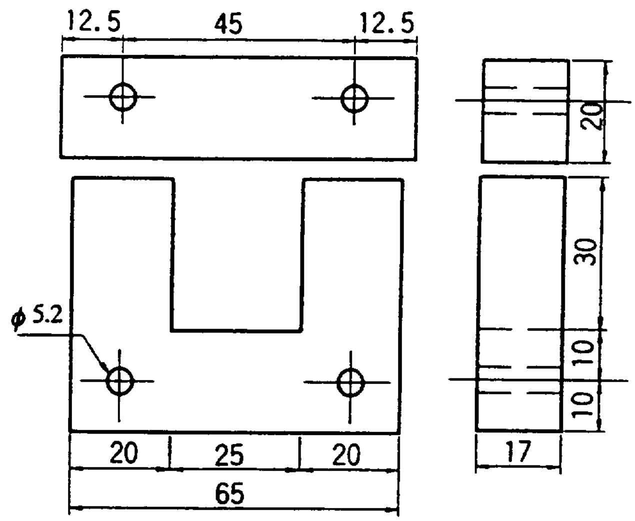

Figure 3. Iron cores of experimental setup

Table 1 Specifications and Data of Experimental Setup

Thickness of iron core	b =17×10^{-3}	m
Width of iron core	a =20×10^{-3}	m
Airgap length	l_a/2=1.0×10^{-3}	m
Permeability of air	μ_o=4π×10^{-7}	H/m
Permeability of iron core	μ=3 000 μ_o	
Conductivity of iron core	σ=1.0×10^{7}	1/Ω•m
Magnet coil: turns	N/2=200	turns/pole
resistance (at 21 ℃)	R_t=1.40	Ω
Mean length of iron core:		
Pole leg	l_1=l_2=30×10^{-3}	m
Connecting stator, Rotor	l_3=l_4=65×10^{-3}	m
Current gain	k_i=0.95	A/V
Control loop gain	p=140	
Time constant	T=0.24×10^{-3}	s
Phase shift	φ=0	rad.
Gain	$\bar{k}_b$=1.0	

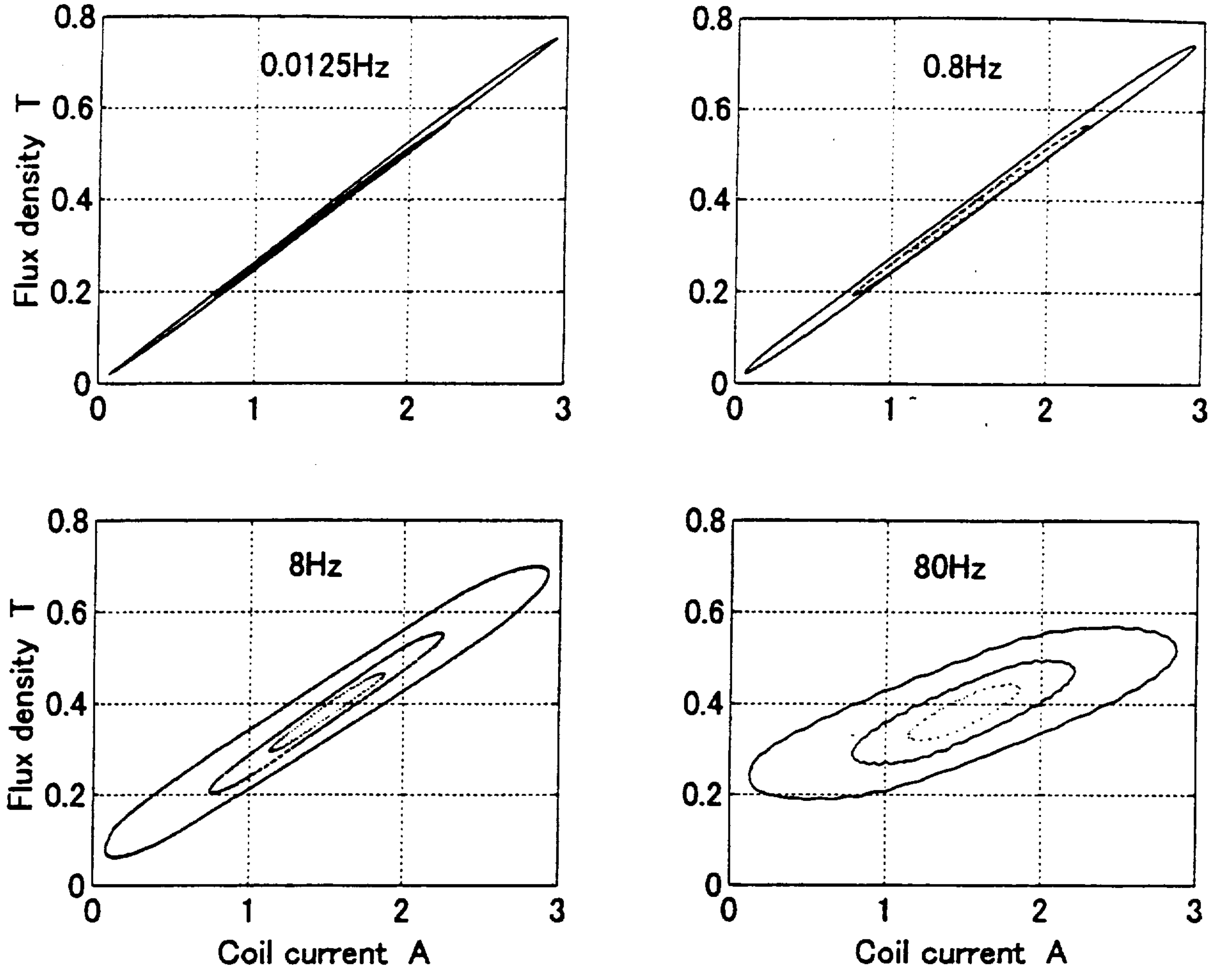

Figure 4. Magnetic hysteresis loop.

We checked that the measurement may be reliable in frequencies below about 100Hz; we measured the hysteresis loops in several frequencies; the results are shown in Fig. 4. We see that the amplitude-dependency of the current-flux gain (k_b in eq. (30)) is very small in low frequencies. In higher frequencies, the loops in each frequency may be similar in shape, but have a larger gradient for a smaller amplitude. The swell of the loop is a result of the time lag mainly due to eddy current effects.

Frequency Response of Flux to Coil-current

The frequency response of magnetic flux to coil current is independent of the characteristics of the power amplifier. To detect the incremental flux, a search coil of two turns was wound around two pole legs, one turn in each, near the pole faces. We input a biasing sinusoidal voltage to the power amplifier, and measured the coil current and the induced voltage between the ends of the search coil to obtain the frequency response between them. From the numerical operation of dividing the response by pure complex numbers $j\omega$, we obtained the response of the incremental flux. The amplitude of the input voltage was taken to give a statical amplitude of the coil current of about 25, 50 and 75% of the bias current. The results are shown by the filled lines in Fig. 5, indicated with the corresponding amplitude of the input voltage. The dependency on the input amplitude is very small in lower frequency; this was

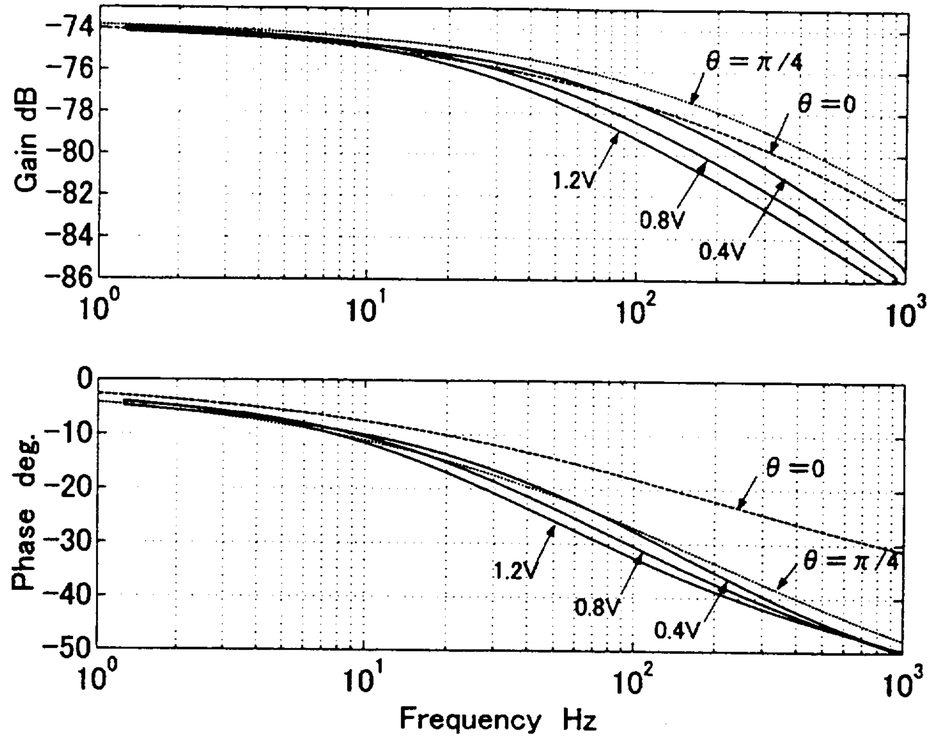

Figure 5. Frequency responses of magnetic flux to coil current.

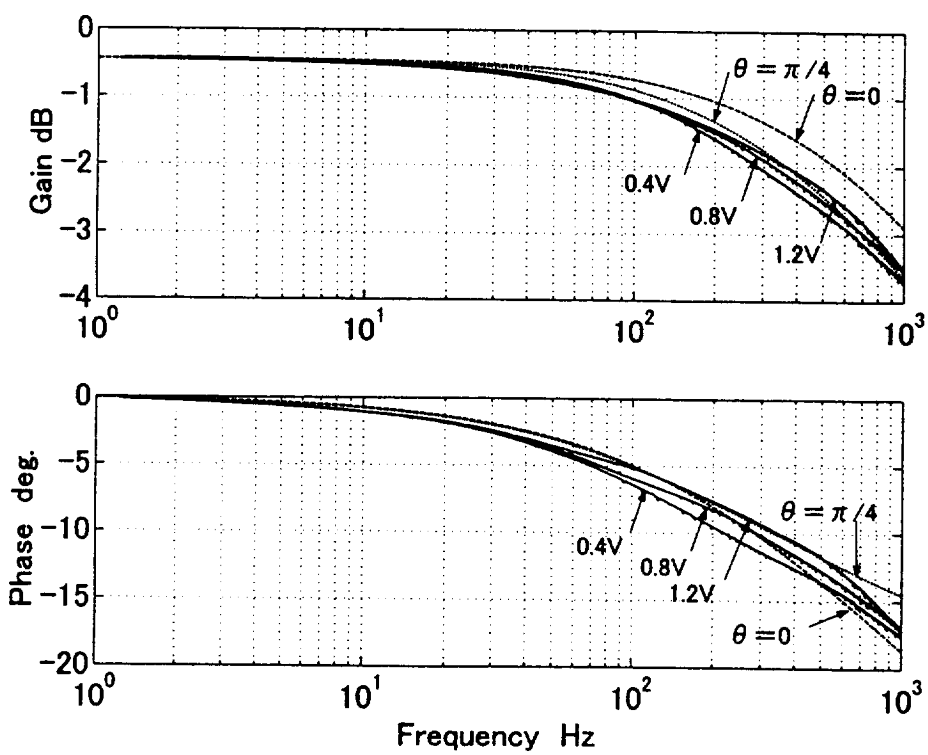

Figure 6. Frequency responses of coil current to input voltage.

expected from the static hysteresis loop. The gain characteristics, however, decays more for a larger amplitude above about 10Hz. This decay is probably because a part of the magnetic flux saturates in some parts of the iron core where the flux takes a short cut.

Numerical results based on eq. (37) with $\bar{k}_b=1$ and $\varphi=0$ are shown in the figure by broken and dotted lines when we assumed $\theta=0$ and $\theta=\pi/4$rad. We shifted these gains up by 2.0dB (1.26 in magnitude) for simplicity of comparison (such a shift is valid because the fringing effect in the working air-gaps increases the flux). With the agreement to the experimental results, the parameter $\theta=0$ gives a better result than $\theta\neq 0$ in the gain , but opposite in the phase. We note that the numerical gain becomes larger for the permeability of a complex number. Anyway, the agreement to the experimental results is unsatisfactory in higher frequencies. This may be mainly due to the flux saturation in the experimental results and also due to defects of the model.

Frequency Response of Coil-current to Input Voltage

The filled lines in Figure 6 shows the experimental frequency responses of coil current to input voltage. The amplitude dependency is much smaller than the response of the flux to the coil current, and the gain increases with input-amplitude in higher frequencies. The latter fact seems contrary to an experience, in general, that the output current decays with the increasing input-amplitude in higher frequencies, as a result of dynamic characteristics of the power amplifier. The experimental result is probably a result of smaller eddy current effects with a smaller magnetic flux.

The broken and dotted lines in the figure show the numerical results of eq. (38). The agreement to the experimental results is much better than the results in Fig. 5; $\theta=\pi/4$rad. Equation (38) may give an explanation for the experimental results with the amplitude dependency, mentioned in the preceding paragraph: the time constant T given by eq. (36) is related to the output amplitude through k_b in eq. (30), and proportional to the output amplitude (gain).

CONCLUSIONS

We presented a simple model in the frequency domain for electromagnetic actuators composed of C-shaped stators of solid iron core with magnetic hysteresis but without leakage flux. The proposed model is described by the half-power of the Laplace transform variable with eddy current effects and a phase shift of the static hysteresis effects in addition to the complex permeability. The agreement to the experimental results is unsatisfactory in higher frequencies. This may be mainly a result of flux saturation in the experiment. Leakage flux may be another factor: the leakage has a little effect on the characteristics of the actuators in lower frequencies, but may be large in higher frequencies.

REFERENCES

1. Aspden, H.: Eddy-Currents in Solid Cylindrical Cores Having Non-Uniform Permeability, *J. Applied Physics*, **23**-5, pp. 523-528, 1952.

2. Kesavamurthy, N., and Rajagopalan, P. K.: Effects of Eddy Currents on the Rise and Decay of Flux in Solid Magnetic Cores, *Proc. IEE*, Vol. 109 C, pp. 63-75, 1961.

3. Subba Rao, V.: Equivalent Circuits of Solid Iron Core for Impact Excitation Problem, *Proc. IEE*, Vol. 111, No. 2, pp. 349-357, 1964.

4. Silvester, P., Eddy Current Models in Linear Solid-Iron Bars, *Proc. IEE*, Vol. 112, No. 8, pp. 1589-1594, 1965.

5. Stoll, R. L.: *The Analysis of Eddy Currents*, pp. 34-40, Clarendon Press, Oxford, 1974.

6. Zmood, R. B., Anand, D. K., and Kirk, J. A.: The Influence of Eddy Currents on Magnetic Actuator Performance, *Proc. IEEE,* **75**-2, pp. 259-260, 1987.

7. Leon, F. de, and Semlyen, A.: Time Domain Modeling of Eddy Current Effects for Transformer Transients, *IEEE Trans. Power Delivery*, **8**-1, pp. 271-277, 1993.

8. Meeker, D. C., Maslen, E. C., and Noh, M. D., An Augmented Circuit Model for Magnetic Bearings Including Eddy Currents, Fringing, and Leakage, *IEEE Trans. Magnetics*, Vol. 32, No. 4, pp. 3219-3227, 1996.

9. Kucera, L., and Ahrens, M.: A Model for Axial Magnetic Bearings Including Eddy Currents, *NASA CP*-3336, *Third Inter. Sympo. on Magnetic Suspension and Technology,* Part 2, pp. 421-436, 1996.

10. Feeley, J. J.: A Simple Dynamic Model for Eddy Currents in a Magnetic Actuators, *IEEE Trans. on Magnetics,* Vol. 32, No. 2, pp. 453-458, 1996.

11. Britcher, C. P., and Bloodgood, D. V.: Eddy Current Influences on the Dynamic Behaviour of Magnetic Suspension Systems, *NASA CP*-1998-207654, *Fourth Inter. Sympo. on Magnetic Suspension and Technology,* pp. 273-284, 1998.

12. Vistin, A. Edit.: *Models of hysteresis*, Longman Scientific & Technical, 1993.